Characteristics of Microbubbles Generated from Perforated Plates

Karakteristik Gelembung Mikro yang Dihasilkan dari Pelat Berlubang

**Dhyna Analyes Trirahayu[1*], Ridwan P. Putra[2], Joshua Mulia Nababan[3],
Mubiar Purwasasmita[4]**

[1]Department of Chemical Engineering, Politeknik Negeri Bandung, Jalan Geger Kalong Hilir,
Bandung, 40559, Indonesia

[2,3,4]Department of Chemical Engineering, Faculty of Industrial Technology, Institut Teknologi Bandung,
Jalan Ganesha 10, Bandung, 40132, Indonesia

Email: [1]dhyna.analyes@polban.ac.id, [2]mg17503@shibaura-it.ac.jp, [3]joshua.mulia992@gmail.com,
[4]mubiar@che.itb.ac.id

*Corresponding Author: **dhyna.analyes@polban.ac.id**

ABSTRAK

Gelembung mikro akhir-akhir ini muncul sebagai media serbaguna dalam berbagai disiplin ilmu dan teknik. Namun, aplikasi gelembung mikro dalam sektor pertanian memerlukan perangkat yang sederhana dan hemat biaya dalam pengoperasiannya. Pada penelitian ini, pendekatan baru untuk memproduksi gelembung mikro dikembangkan menggunakan pelat berlubang yang digabungkan dengan kolom kaca. Dua jenis pelat dengan jumlah lubang yang berbeda telah difabrikasi untuk memproduksi gelembung mikro. Karakterisasi gelembung mikro yang dihasilkan menunjukkan bahwa diameter gelembung mikro yang diproduksi berkisar antara 10,4 hingga 21,1 µm. Rasio gas-cair yang dihasilkan cenderung meningkat sebesar 30-40%, dengan meningkatnya laju alir gas oksigen dan durasi pengaliran gas. Selain itu, peningkatan laju alir gas oksigen dan durasi pengaliran gas juga dapat memperpanjang waktu tinggal gelembung mikro. Secara umum, teknik ini cukup menjanjikan untuk diterapkan di sektor pertanian, terutama pada sistem penanaman hidroponik.

Kata kunci: *gelembung mikro, pelat berlubang, laju alir gas, durasi pengaliran gas, waktu tinggal.*

ABSTRACT

Microbubbles are emerging as versatile tools in numerous scientific and engineering disciplines. However, the applications of microbubbles in agricultural fields require a simple and cost-effective device that can be used to generate microbubbles. In this study, a new approach to producing microbubbles was developed using perforated plates incorporated with glass columns. Two different plates with various numbers of holes were fabricated. Characterization of the microbubbles showed that the diameter of the microbubbles produced was in the range of 10.4 to 21.1 µm. The gas-liquid ratio tended to increase by around 30-40%, with increasing oxygen gas flow rate and gas-jetting time. The enhanced oxygen gas flow rate and gas-jetting time also prolonged the residence time of the microbubbles. In general, this technique is promising that can be implemented in agricultural sectors, especially in hydroponic systems.

Keywords: microbubbles, perforated plates, gas flow rate, gas-jetting time, residence time

1. INTRODUCTION

Microbubbles are defined as bubbles that have diameters less than 50 µm (Muroyama et al., 2013). The microbubbles have been widely applied in various engineering and scientific applications. In biomedical fields, microbubbles are employed in drug and gene delivery along with ultrasound (Unger et al., 2014). Protein microbubbles are utilized as structural elements to control texture in the food industry, allowing the manufacture of healthier foods with increased consumer acceptance (Rovers et al., 2016). Floatation of fine particles in the mining industry can also be performed using microbubbles due to longer residence time and increased surface area, hence enhancing the particle-bubble collision probability (Santana et al., 2012).

Wastewater treatment using air and ozone microbubbles can vastly reduce the total suspended solids, biological oxygen demand, and chemical oxygen demand in the samples (Wen et al., 2011).

In agricultural sectors, the development of ozone microbubbles is promising to remove residual pesticide present in vegetables. The ozone microbubbles can easily infiltrate into vegetables with various shapes that can interact with pesticide molecules (H. Ikeura et al., 2011). Recently, the effect of microbubbles in deep flow hydroponic culture was also studied to enhance spinach growth. The study reveals that the microbubbles can promote the growth of spinach with a maintained high dissolved oxygen level (Hiromi Ikeura et al., 2017). In another study, microbubbles were employed to foster the growth of iceberg lettuce in hydroponic systems. The results indicate that the application of microbubbles in the hydroponic system can significantly enhance plant growth and increase secondary metabolite and antioxidant levels (Abu-Shahba et al., 2021).

Many techniques have been implemented to generate microbubbles. Makuta et al. introduced the generation of microbubbles with 100 µm diameter using a hollow cylindrical ultrasonic horn. The formation of microbubbles from the horn demands a higher ultrasonic power input, with a maximum yield of bubble generation increasing with the increase of gas flow rate (Makuta et al., 2013). Flow-focusing microfluidic devices also offer an effective solution to enable in situ generations of microbubbles which can control diameters accurately in real-time. Complex manifolds and unrequired tubing interconnects are eliminated by coupling the device with a chamber containing a pressurized liquid (Dhanaliwala et al., 2013). However, due to the complication in designing such devices, a simple instrument that can be used to generate microbubbles at a low cost is required.

In this work, we introduced a simple and cost-effective technique to generate microbubbles using perforated plates. The plates were prepared from molded silicon rubber resin and perforated using a guitar string. Two different plates with different numbers of holes were fabricated. The plates were employed as supports of columns to study the characteristics of the microbubbles generated. The size of microbubbles produced from the perforated plates was estimated. The effects of volumetric gas flow rate on gas-liquid ratio and microbubble residence time were studied. In addition, the effects of gas-jetting time on gas-liquid ratio and microbubble residence time were investigated. To the best of our knowledge, this study is the first to report a simple method to generate microbubbles using perforated plates that can be applied in agricultural sectors.

2. MATERIALS AND METHODS

2.1. Materials

Guitar strings with a diameter of 210 µm were used to generate the micro-sized holes where the microbubbles were produced. Epoxy resin was utilized to mold support plates with micro-sized holes. Methyl ethyl ketone peroxide (MEKP) as catalyst was involved in accelerating the resin hardening process. Oxygen was utilized as the gas source to generate the microbubbles. Demineralized water was used as the medium where the microbubbles were formed..

2.2. Plate Molding

Two support plates with different numbers of micro-sized holes were fabricated using silicon rubber resin (Figure 1). One hole was generated on the first plate (GS1), while four holes were created on the second plate (GS4). To prepare the support plates, rubber resin was poured into two molders. The first molder was perforated using one guitar string, while the second molder was penetrated with four guitar strings. The catalyst was subsequently added into the resin to speed up the resin hardening process. After the resin solidified, the guitar strings were removed from the plates. The plates were then used as supports in glass columns.
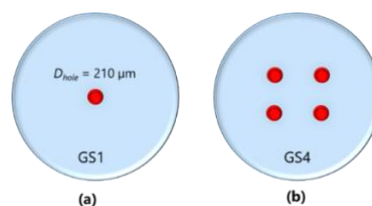
Figure-1. Scheme of column support plates with (a) one micro-sized hole (GS1) and (b) four micro-sized holes (GS4) to generate microbubbles

2.3. Experimental Set-Up

The microbubbles were generated using a glass column filled with demineralized water, as shown in Figure 2. The support plates with micro-sized holes were placed at the bottom of the columns. The column was connected with an oxygen tank equipped with a pressure gauge to monitor the pressure inside the oxygen tank. A rotameter was placed between the column and the oxygen tank to control the oxygen gas flow rate.
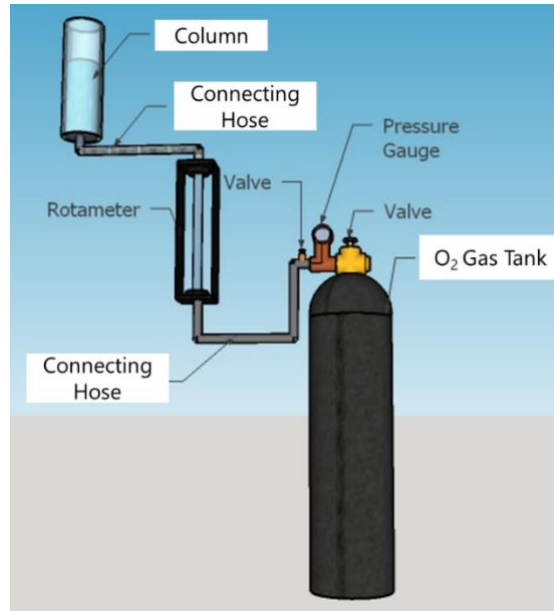
Figure-2. Experimental set-up of microbubble generation from perforated plates in a glass column filled with demineralized water

2.4. Microbubble Generation

Demineralized water was poured into the column to reach a water level of 3 cm. The effects of volumetric oxygen gas flow rate on gas-liquid ratio and microbubble residence time were investigated by controlling the oxygen gas flow rate using the rotameter. Various oxygen gas flow rates were applied: 0.3, 0.4, 0.5, 0.6, 0.7, and 0.8 mL/s. The effects of gas-jetting time on gas-liquid ratio and microbubble residence time were studied. Different gas-jetting times were implemented: 180, 360, 540, 720, and 900 s. The microbubble diameter (D) was calculated using Stokes' Law for spherical bubbles as justified in Equation (1) and rearranged to yield Equation (2).

$$V_{ts} = \frac{gD^2(\rho-\rho_a)}{18\eta} \tag{1}$$

$$D = \sqrt{\frac{18V_{ts}\eta}{g(\rho-\rho_a)}} \tag{2}$$

Where V_{ts} is the bubble rise velocity, g is the gravitational acceleration, ρ is the density of water, ρ_a is the density of oxygen gas, and η is the viscosity of water. The Equation (2) can be applied to estimate the size of a microbubble with a bubble diameter of 1-100 µm (Andreev et al., 2019).

3.   RESULTS AND DISCUSSION
3.1. Size of Generated Microbubbles

The diameters of microbubbles were estimated using Stokes' Law as stated in Equation (2). The average microbubble diameters measured at different oxygen flow rates produced from the GS1 and GS4 plate are summarized in Table 1. The results indicated that the increase of oxygen flow rate induced the rise of the microbubble size. These are relevant to Stokes' Law equation that shows a linear correlation between bubble rise velocity and square of bubble diameter. The increase of gas flow rate influences the rise of bubble rise

velocity. The transition from homogenous to heterogeneous flow is considered a gradual process (Sarhan et al., 2018). The bubble diameters obtained from this study satisfy the specification of a microbubble. A microbubble is defined as a bubble that possesses a diameter less than approximately 50 µm (Muroyama et al., 2013).

In another study on hydroformylation of 1-hexene in microbubble media conducted by Peng et al., the average microbubble diameter rises as the gas flow rate increases from 20 to 40 mL/min. The study implies that a gas flow rate of 30 mL/min is the optimum gas feeding rate. The employment of a fractal generator can generate smaller microbubbles with a more uniform distribution (Peng et al., 2020). The results agree with a study on the bubble formation in a continuous liquid phase under industrial jetting conditions. The study shows that the bubble size initially increases monotonously to reach a specific value and then stays nearly constant as the gas velocity increases (Xiao et al., 2019).

Table-1. Average diameters of microbubbles at different oxygen gas flow rates estimated using Stokes' Law equation produced from GS1 and GS4 plate

Gas Flow rate (mL/s)	Average Bubble Diameter (µm)	
	GS1	GS4
0.3	10.4	17.6
0.4	13.5	19.0
0.5	13.6	19.7
0.6	15.1	19.0
0.7	16.3	21.1

3.2. Effect of Oxygen Gas Flow Rate On Gas-Liquid Ratio

The effect of oxygen gas flow rate on the gas-liquid ratio in the column was investigated by varying the oxygen gas flow rates using the rotameter. The relationships between the gas-liquid ratio vs. the gas oxygen flow rate in the columns with the GS1 and GS4 perforated plate configurations are presented in Figure 3. The results indicated that the gas-liquid ratio tended to be constant at 0.1 within a flow rate range of 0.3 to 0.6 mL/s and significantly increased to 0.13 at a flow rate of 0.8 mL/s in the column with the GS1 plate. Meanwhile, the gas-liquid ratio in the column with the GS4 plate rose from 0.03 to 0.05 at a flow rate range of 0.3-0.4 mL/s to 0.5-0.7 mL/s. The gas-liquid ratio subsequently returned to 0.03 at a flow rate of 0.8 mL/s. In another study on a microbubble generator and microbubble generation device, a lower gas flow rate results in a smaller microbubble size and more number of microbubbles generated (Hato, 2015). The inlet pressure and nozzle distance have a crucial influence on the gas-liquid ratio (Wang et al., 2021).

It was also noticed that the gas-liquid ratios in the column with the GS1 plate were considerably higher than the values with the GS4 plate. These were expected due to a more focused oxygen gas flow because of the presence of merely one micro hole in the GS1 plate. With only one micro hole, the oxygen gas pressure was immense that led to the gas-liquid ratio enhancement. The increase in the gas pressure induces more gas solubility, indicated by the enhanced gas-liquid ratio. This increase can be insignificant when the saturated solubility is reached (Zhao et al., 2016). At a constant temperature condition, the increase in supplied air pressure also raises the diameter of air jets emerging from elastic orifices (Mezhericher et al., 2016). A larger microbubble size is likely to increase the gas-liquid ratio in the column.
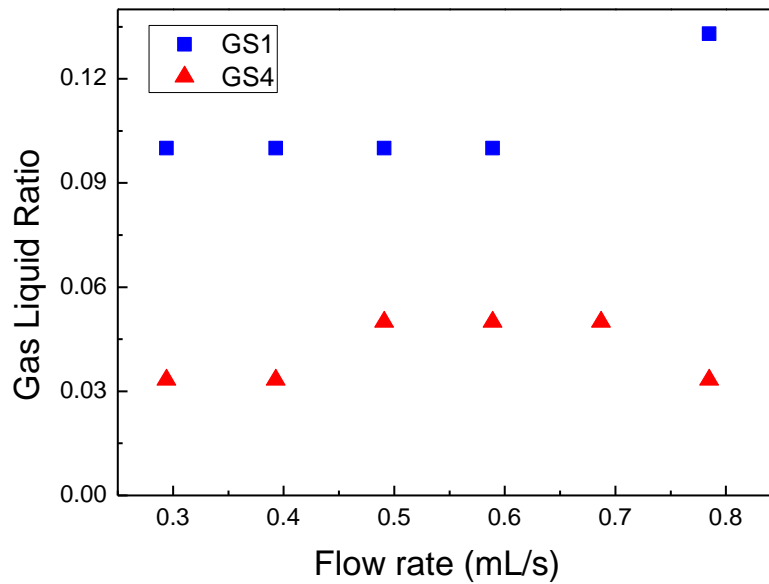
Figure-3. Effect of oxygen gas flow rate on gas-liquid ratio from GS1 and GS4 perforated plates

3.3. Effect of Oxygen Gas Flow Rate on Microbubble Residence Time

The effect of oxygen gas flow rate on the microbubble residence time in the columns with the GS1 and GS4 perforated plate configurations are depicted in Figure 4. The results showed that the increase in the oxygen gas flow rate was likely to prolong the microbubble residence time in the columns. The higher oxygen gas flow rate resulted in a higher microbubble size (Table 1) which was responsible for the increased residence time. Similar results were observed upon the study of bubble behavior of NH_3-H_2O bubble absorption. The study indicates that the residence time rises with the increase of initial bubble diameter in the corresponding liquid concentration (Kang et al., 2002). In another study on the residence time of air bubbles <400 µm diameter at distilled water and seawater surfaces, the residence time is also found to increase with size. The residence time reaches 0.3 s for the bubbles with a diameter of 300 µm. Bubble collisions are likely to occur in seawater to produce coalescence when the bubbles are less than 80 µm diameter (Struthwolf & Blanchard, 1984).
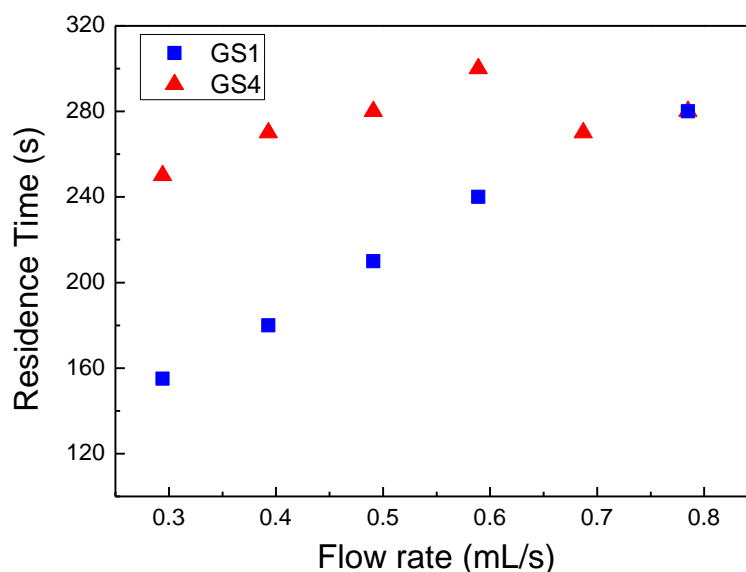

Figure-4. Effect of oxygen gas flow rate on residence time of microbubbles generated from GS1 and GS4 perforated plates

From Figure 4, at a flow rate range of 0.3 to 0.6 mL/s, the residence time of microbubbles in the column with the GS4 plate was higher than those with the GS1 plate. With four microholes in the GS4 plate, more microbubbles were generated in the column, which were responsible for the extended residence time. The microbubbles produced from the GS4 plate were more likely to collide to yield larger microbubbles that were the cause of prolonged residence time (Struthwolf & Blanchard, 1984).

3.4. Effect of Oxygen Gas-Jetting Time on Gas-Liquid Ratio

Different gas-jetting times were implemented to study the effects of gas-jetting time on the gas-liquid ratio. The relationships between the gas-liquid ratio vs. the gas-jetting time in the columns with the GS1 and GS4 perforated plate configurations are shown in Figure 5. The experiments showed that the gas-liquid ratio in the column with the GS1 plate remained constant at 0.1 with a gas-jetting time of 180 to 720 s. The value increased to 0.12 upon 900 s of oxygen gas flow. Meanwhile, the gas-liquid ratio in the column with the GS4 plate increased from 0.03 to 0.05 upon flowing with oxygen gas for 180 to 360 s. The value stayed monotonously and increased to 0.07 with a gas-jetting time of 900 s. The phenomena were likely due to more oxygen gas dissolved in the water upon prolonged gas-jetting duration. In the study on concentration changes of CO_2 in 1-(2-hydroxyethyl) piperidine aqueous solution, the total CO_2 concentration increases from 0 to 1.70 mol/L upon 50 min of CO_2 bubbling (Furukawa et al., 2017). This implies that prolonged gas-jetting time results in more gas supplied into the solution, which induces a higher gas-liquid ratio.

The gas-liquid ratios in the column with the GS1 plate were significantly higher than those with the GS4 plate. With only one microhole in the GS1 plate, the oxygen gas pressure was higher, which resulted in the gas-liquid ratio enhancement. The increase in the gas pressure induces more gas solubility along with the prolonged gas-jetting time (Zhao et al., 2016).
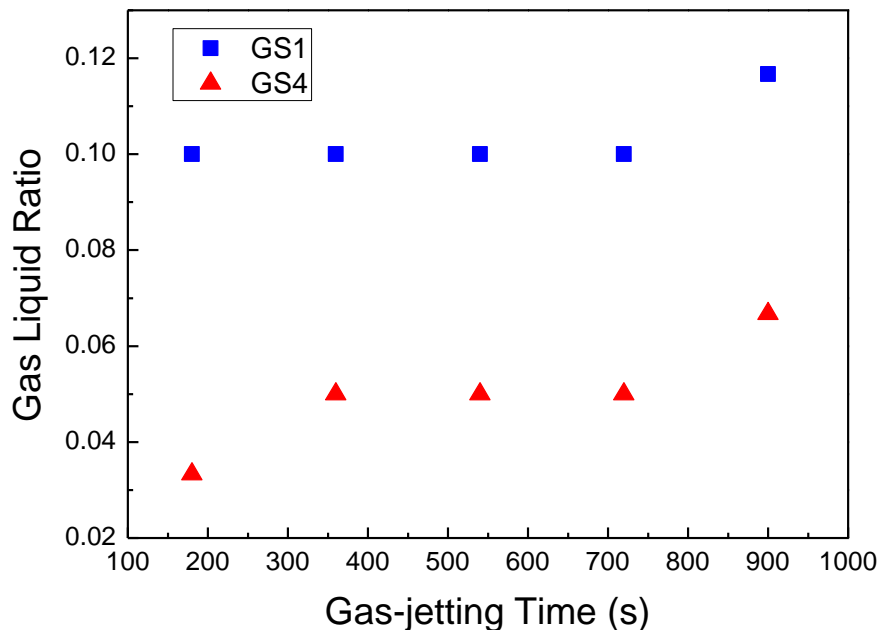
Figure-5. Effect of oxygen gas-jetting time on gas-liquid ratio from GS1 and GS4 perforated plates

3.5. Effect of Oxygen Gas-Jetting Time on Microbubble Residence Time

The effect of oxygen gas-jetting time on the microbubble residence time in the columns with the GS1 and GS4 perforated plate configurations are presented in Figure 6. The results indicated that the extended gas-jetting time resulted in the prolonged microbubble residence time. These trends were likely due to more microbubbles produced in the water with prolonged oxygen gas-jetting time. In addition, larger microbubbles formed with increasing gas-jetting time required longer time to travel to the water surface (Struthwolf & Blanchard, 1984).
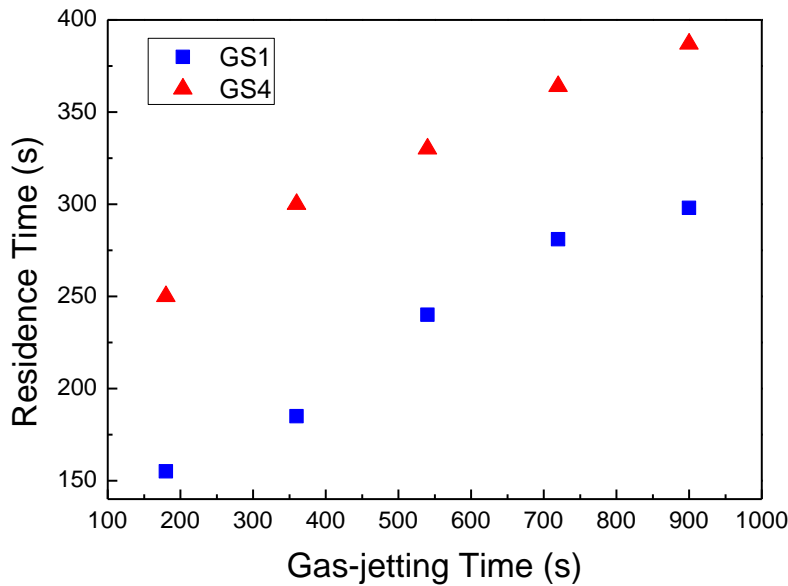
Figure-6. Effect of oxygen gas-jetting time on residence time of microbubbles generated from GS1 and GS4 perforated plates

The column with the GS4 plate showed longer microbubbles residence time than that with the GS1 plate. The phenomena were expected due to more microbubbles generated by the GS4 column colliding to form larger microbubbles. These large microbubbles needed more time to rise to the surface. According to the study on stochastic induction time of attachment due to the formation of transient holes in the intervening water films between air bubbles and solid surfaces, the time required for a bubble to move within a distance of ho is indicated by the Stefan-Reynolds equation (Li et al., 2020).

4. **CONCLUSION**

In summary, a simple and cost-effective approach to producing microbubbles was developed using perforated plates incorporated into a column. Characterization of the microbubbles showed that the diameter of the microbubbles generated using this method was in the range of 10.4 to 16.3 µm, measured at a feed gas flow rate of 0.3 to 0.7 mL/s. The gas-liquid ratio tended to increase with increasing oxygen gas flow rate from both the GS1 and GS4 plates. The gas-liquid ratios in the column with the GS1 plate was considerably higher than those with the GS4 plate due to a more focused oxygen flow rate with only one microhole. The increase in the oxygen gas flow rate and gas-jetting time prolonged the microbubbles residence time in the columns because of larger microbubble sizes produced. The column with the GS4 plate generated more microbubbles that had the tendency to collide with one another. The gas-liquid ratio and microbubble residence time increased with increasing gas-jetting time because more oxygen gas dissolved in the water with prolonged gas-jetting duration. Moreover, more numbers of microbubbles with larger sizes were produced with extended gas-jetting time. Larger microbubbles require a longer time to travel to the water surface. Overall, this technique is promising and can be applied in agricultural sectors, especially in hydroponic systems.

REFERENCES
Abu-Shahba, M. S., Mansour, M. M., Mohamed, H. I., & Sofy, M. R. (2021). Comparative Cultivation and Biochemical Analysis of Iceberg Lettuce Grown in Sand Soil and Hydroponics With or Without Microbubbles and Macrobubbles. *Journal of Soil Science and Plant Nutrition*, *21*(1), 389–403. https://doi.org/10.1007/s42729-020-00368-x
Andreev, S. Y., Garkina, I. A., & Yakhkind, M. I. (2019). Evaluating the patterns of air bubble rise in water-air mixtures used in natural and waste water treatment processes. *IOP Conference Series: Materials Science and Engineering*, 066054. https://doi.org/10.1088/1757-899X/687/6/066054

Dhanaliwala, A. H., Chen, J. L., Wang, S., & Hossack, J. A. (2013). Liquid flooded flow-focusing microfluidic device for in situ generation of monodisperse microbubbles. *Microfluidics and Nanofluidics*, *14*(3–4), 457–467. https://doi.org/10.1007/s10404-012-1064-x

Furukawa, Y., Koriki, H., Shuto, D., Sato, H., & Yamanaka, Y. (2017). 13C-NMR Study of Acid Dissociation Constant (pKa) Effects on the CO2 Absorption and Regeneration of Aqueous Alkanolpiperidine. *Energy Procedia*, *114*, 1765–1771. https://doi.org/10.1016/j.egypro.2017.03.1304

Hato, Y. (2015). *Micro-bubble generator and micro-bubble generation device* (Patent No. US 8991796B2). U.S. Patent. https://patentimages.storage.googleapis.com/80/6b/90/e129e1ac6556a0/US8991796.pdf

Ikeura, H., Kobayashi, F., & Tamaki, M. (2011). Removal of residual pesticide, fenitrothion, in vegetables by using ozone microbubbles generated by different methods. *Journal of Food Engineering*, *103*(3), 345–349. https://doi.org/10.1016/j.jfoodeng.2010.11.002

Ikeura, Hiromi, Tsukada, K., & Tamaki, M. (2017). Effect of microbubbles in deep flow hydroponic culture on Spinach growth. *Journal of Plant Nutrition*, *40*(16), 2358–2364. https://doi.org/10.1080/01904167.2017.1346663

Kang, Y. T., Nagano, T., & Kashiwagi, T. (2002). Visualization of bubble behavior and bubble diameter correlation for NH3–H2O bubble absorption. *International Journal of Refrigeration*, *25*(1), 127–135. https://doi.org/10.1016/S0140-7007(00)00045-1

Li, S., Nguyen, A. V., & Sun, Z. (2020). Stochastic induction time of attachment due to the formation of transient holes in the intervening water films between air bubbles and solid surfaces. *Journal of Colloid and Interface Science*, *565*, 345–350. https://doi.org/10.1016/j.jcis.2020.01.027

Makuta, T., Suzuki, R., & Nakao, T. (2013). Generation of microbubbles from hollow cylindrical ultrasonic horn. *Ultrasonics*, *53*(1), 196–202. https://doi.org/10.1016/j.ultras.2012.05.010

Mezhericher, M., Ladizhensky, I., Mazor, G., & Etlin, I. (2016). Formation of Dry Fog from Thin Liquid Films Disintegrated by Gas Jets. *ILASS – Europe 2016, 27th Annual Conference on Liquid Atomization and Spray Systems*.

Muroyama, K., Imai, K., Oka, Y., & Hayashi, J. (2013). Mass transfer properties in a bubble column associated with micro-bubble dispersions. *Chemical Engineering Science*, *100*, 464–473. https://doi.org/10.1016/j.ces.2013.03.043

Peng, F., Zhang, J., Tang, Z., & Sun, Y. (2020). Enhanced hydroformylation of 1-hexene in microbubble media. *Asia-Pacific Journal of Chemical Engineering*, *15*(4), e2484. https://doi.org/10.1002/apj.2484

Rovers, T. A. M., Sala, G., van der Linden, E., & Meinders, M. B. J. (2016). Effect of Temperature and Pressure on the Stability of Protein Microbubbles. *ACS Applied Materials & Interfaces*, *8*(1), 333–340. https://doi.org/10.1021/acsami.5b08527

Santana, R. C., Ribeiro, J. A., Santos, M. A., Reis, A. S., Ataíde, C. H., & Barrozo, M. A. S. (2012). Flotation of fine apatitic ore using microbubbles. *Separation and Purification Technology*, *98*, 402–409. https://doi.org/10.1016/j.seppur.2012.06.014

Sarhan, A. R., Naser, J., & Brooks, G. (2018). CFD modeling of bubble column: Influence of physico-chemical properties of the gas/liquid phases properties on bubble formation. *Separation and Purification Technology*, *201*, 130–138. https://doi.org/10.1016/j.seppur.2018.02.037

Struthwolf, M., & Blanchard, D. C. (1984). The residence time of air bubbles <400 μm diameter at the surface of distilled water and seawater. *Tellus B: Chemical and Physical Meteorology*, *36*(4), 294–299. https://doi.org/10.3402/tellusb.v36i4.14911

Unger, E., Porter, T., Lindner, J., & Grayburn, P. (2014). Cardiovascular drug delivery with ultrasound and microbubbles. *Advanced Drug Delivery Reviews*, *72*, 110–126. https://doi.org/10.1016/j.addr.2014.01.012

Wang, C., Wang, C., Yu, A., Zheng, M., & Khan, M. S. (2021). Effect of Closure Characteristics of Annular Jet Mixed Zone on Inspiratory Performance and Bubble System. *Processes*, *9*(8), 1392. https://doi.org/10.3390/pr9081392

Wen, L. H., Ismail, A. Bin, Menon, P. M., Saththasivam, J., Thu, K., & Choon, N. K. (2011). Case studies of microbubbles in wastewater treatment. *Desalination and Water Treatment*, *30*(1–3), 10–16. https://doi.org/10.5004/dwt.2011.1217

Xiao, H., Geng, S., Chen, A., Yang, C., Gao, F., He, T., & Huang, Q. (2019). Bubble formation in continuous liquid phase under industrial jetting conditions. *Chemical Engineering Science*, *200*, 214–224. https://doi.org/10.1016/j.ces.2019.02.009

Zhao, B., Tao, W., Zhong, M., Su, Y., & Cui, G. (2016). Process, performance and modeling of CO2 capture

by chemical absorption using high gravity: A review. *Renewable and Sustainable Energy Reviews*, *65*, 44–56. https://doi.org/10.1016/j.rser.2016.06.059